Astron. Astrophys. 292, 125–132 (1994)

ASTRONOMY AND ASTROPHYSICS

Λ-quenching as the nonlinearity in stellar-turbulence dynamos

L.L. Kitchatinov[1,2], **G. Rüdiger**[1], **and M. Küker**[1]

[1] Astrophysikalisches Institut Potsdam, An der Sternwarte 16, D-14482 Potsdam, Germany
[2] Institute for Solar-Terrestrial Physics, P.O. Box 4026, Irkutsk, 664033, Russia

Received 18 December 1993 / Accepted 18 June 1994

Abstract. A novel scenario for the nonlinear stellar dynamo is presented. Differential rotation in solar-type stars is assumed as due to the influence of the global rotation upon anisotropic turbulence ("the Λ-effect"). The effect, however, is quenched by the dynamo-induced large-scale magnetic fields. The resulting reduction of the differential rotation feeds back on the dynamo itself.

Both the derivation of the Λ-quenching expressions as well as a (simplified) dynamo model are presented. The dynamo equation is completed with the equation for the radial differential rotation. The phase relation between both the components of the magnetic field *and* the slope in the rotation law is essential for the temporal behaviour of the dynamo magnetism. Both the observational phenomena of solar torsional oscillations as well as the Maunder minimum are covered by the theory.

Key words: magnetohydrodynamics – turbulence – stars: rotation – stars: magnetic fields – stars: interiors

1. Motivation

For several problems of stellar physics it proves to be important to find the magnetic influence on the rotation law in outer convection zones. It is directly observed in form of the solar "torsional oscillations", i.e. an equatorwards migrating pattern of belts of slow and fast rotation (Howard & LaBonte 1980). Old theoretical explanations are based on the calculations of the dynamo-originated mean-field Lorentz force – also known as the Malkus-Proctor effect (Malkus & Proctor 1975).

Since the pioneering paper by Noyes, Weiss & Vaughan (1984) this effect is assumed to be responsible for the Rossby number dependence of the frequency $\omega_{\rm cyc}$ of observed stellar activity cycles. Nonlinear dynamo waves have been considered which yield a sufficiently high exponent $\hat{n} = \partial \log \omega_{\rm cyc} / \partial \log |\mathscr{D}|$ with $\mathscr{D}$ as the dynamo number only under inclusion of the time-dependence of the rotation shear $\partial\Omega/\partial x$.

Send offprint requests to: G. Rüdiger

It is, however, not obvious that mainly the mean-field Lorentz force $\mathrm{rot}\,\overline{\boldsymbol{B}} \times \overline{\boldsymbol{B}}$ modifies the rotation law. There is also the possibility that the Λ-effect is effectively influenced by the magnetic field. The Λ-effect is the turbulent driver of the differential rotation (Rüdiger 1989). It results from the fact that in an anisotropic turbulence field even a uniform rotation transports angular momentum. It can be determined by computing the rotational influence on the off-diagonal elements of the total Reynolds stress tensor.

If simultaneously the magnetic influence on the Reynolds stress is considered one finds the effect of Λ-quenching. In contrasts to the Malkus-Proctor effect the Λ-quenching effectivity runs with the magnetic energy density, $\overline{B}^2$. As in $\alpha\Omega$-dynamos the energy is dominated by toroidal fields, it has been argued that Λ-quenching might be more effective in producing torsional oscillations than the Malkus-Proctor effect (Kitchatinov 1990; Rüdiger & Kitchatinov 1990).

For the magnetic quenching of the differential rotation Jennings & Weiss (1991) worked with a heuristic ansatz of the induced magnetic field,

$$\frac{\partial\Omega}{\partial x} \propto \frac{\tilde{\Omega}_0}{1+\kappa\overline{B}^2}. \qquad (1)$$

The related nonlinear solutions of 1D $\alpha\Omega$-dynamo models exhibit a distinct spatial North-South-asymmetry.

Previously published studies of nonlinear dynamos yielded stable solutions with dipole and quadrupole parity as well as mixed-mode solutions (Brandenburg et al. 1989; Schmitt & Schüssler 1989). Solar observations show indeed that the surface magnetism has a (weak) N-S-asymmetry (Stenflo & Vogel 1986). After Ribes & Nesme-Ribes (1993) such an asymmetry even dominated during the Maunder minimum. Already Spörer (1889) reported that all but two sunspots recorded between 1671 and 1713 were in the southern hemisphere.

In the Maunder minimum we encounter a number of interesting phenomena. Together with the basic low-energy state there is a clear N-S-asymmetry of the magnetic activity and a strikingly enhanced differential rotation (Ribes & Nesme-Ribes 1993). All facts together are forming the mystery of the Maunder minimum.

Nonlinear 2D shell-dynamo models with magnetic feedback on the large-scale flow are described by Brandenburg et al. (1990). Parity mixing and long-term magnetic weakening indeed occur in $\alpha\Omega$-dynamos in outer convection zones but the critical dynamo numbers for even and odd parity lie very close together and the differences in the related magnetic cycle periods are very small. The period of the mixed solutions is then very long compared to the period of the basic magnetic cycle.

The interpretation of the occurence of a second frequency in terms of the Maunder minimum thus comes into trouble for dynamos in relatively thin shells.

In the present paper we shall develop a dynamo theory with magnetic quenching of differential rotation included. The theoretical background for the rotation-law theory can be found in Kitchatinov & Rüdiger (1993, Paper I).

2. Basic equations

The zonal momentum fluxes in rotating turbulent fluids are proportional to the off-diagonal components of the turbulent stress tensor T_{ij}. Both Reynolds and Maxwell stresses must be included to find the magnetic field influence on the angular momentum transport: $T_{ij} = \rho\langle u'_i u'_j\rangle - \langle B'_i B'_j\rangle/\mu$. We kept the Second-order Correlation Approximation (SOCA) to derive the stresses. The equations for the fluctuating fields are used in their linearised form. In particular, the equation for the velocity, $\boldsymbol{u}'$, reads

$$\partial\boldsymbol{u}'/\partial t + \rho^{-1}\nabla\left(p' + (\overline{\boldsymbol{B}}\cdot\boldsymbol{B}')/\mu\right) - (\overline{\boldsymbol{B}}\cdot\nabla)\boldsymbol{B}'/(\mu\rho) + 2\,\boldsymbol{\Omega}\times\boldsymbol{u}' - \nu_t\Delta\boldsymbol{u}' = \boldsymbol{f}'/\rho, \quad (2)$$

where ν_t is the effective viscosity due to micro-turbulence, p' the fluctuating pressure, and $\boldsymbol{f}'$ is the random body force driving the turbulence. We prescribe the random force $\boldsymbol{f}'$ as the turbulence driver instead of addressing the rather complicated problem of thermal convection. We assume further the fluid to be incompressible,

$$\mathrm{div}\,\boldsymbol{u}' = 0. \quad (3)$$

It is advantageous to use Fourier-transformed equations. From (2) we get

$$(\nu_t k^2 - i\omega)\hat{\boldsymbol{u}} - i(\boldsymbol{k}\cdot\overline{\boldsymbol{B}})\hat{\boldsymbol{B}}/(\mu\rho) + 2(\boldsymbol{k}^\circ\cdot\boldsymbol{\Omega})\,\boldsymbol{k}^\circ\times\hat{\boldsymbol{u}} = \hat{\boldsymbol{f}}^s/\rho, \quad (4)$$

where the pressure has been eliminated by using (3), $\boldsymbol{k}^\circ = \boldsymbol{k}/k$ is the unit vector, $\boldsymbol{f}^s$ is the solenoidal part of the force and Fourier-amplitudes are defined by hats:

$$\boldsymbol{u}'(\boldsymbol{r},t) = \int \hat{\boldsymbol{u}}(\boldsymbol{k},\omega)e^{i(k\cdot r-\omega t)}\,d\boldsymbol{k}\,d\omega. \quad (5)$$

We also need the expression for the fluctuating magnetic field,

$$\hat{\boldsymbol{B}} = \frac{i(\boldsymbol{k}\cdot\overline{\boldsymbol{B}})\hat{u}}{\eta_t k^2 - i\omega}. \quad (6)$$

Substitution of (6) into (4) gives the equation for the velocity amplitude,

$$N\hat{\boldsymbol{u}} + \frac{2(\boldsymbol{k}^\circ\cdot\boldsymbol{\Omega})}{\nu_t k^2 - i\omega}\,\boldsymbol{k}^\circ\times\hat{\boldsymbol{u}} = \hat{\boldsymbol{u}}^{(0)}, \quad (7)$$

where

$$N = 1 + \frac{(\boldsymbol{k}\cdot\boldsymbol{V})^2}{(\nu_t k^2 - i\omega)(\eta_t k^2 - i\omega)}. \quad (8)$$

$\boldsymbol{V} = \overline{\boldsymbol{B}}/\sqrt{\mu\rho}$ is the Alfvèn velocity, $\hat{\boldsymbol{u}}^{(0)} = \hat{\boldsymbol{f}}^s/\rho(\nu_t k^2 - i\omega)$ is the velocity amplitude for the 'original turbulence' which is imagined to exist in a non-rotating non-magnetised fluid.

From Eq. (7) the usual linear relation

$$\hat{u}_i = D_{ij}\hat{u}^{(0)}_j, \quad (9)$$

can be found wherein the tensor

$$D_{ij} = \frac{N\delta_{ij} + \frac{2(k^\circ\cdot\Omega)}{\nu_t k^2 - i\omega}\epsilon_{ijp}k^\circ_p}{N^2 + \frac{4(k^\circ\cdot\Omega)^2}{(\nu_t k^2 - i\omega)^2}} \quad (10)$$

accounts for the influence of the global rotation and the mean magnetic field. For slow rotation Eq. (10) simplifies to

$$D_{ij} = N^{-1}\left[\delta_{ij} + \frac{2(\boldsymbol{k}^\circ\cdot\boldsymbol{\Omega})}{N(\nu_t k^2 - i\omega)}\epsilon_{ijs}k^\circ_s\right]. \quad (11)$$

For the case of weak fields (but arbitrary rotation) it is

$$D_{ij} = D^{(\circ)}_{ij} + \frac{(\boldsymbol{k}\cdot\boldsymbol{V})^2}{(\nu_t k^2 - i\omega)(\eta_t k^2 - i\omega)}\frac{1}{M}\left(\delta_{ij} - 2D^{(\circ)}_{ij}\right) \quad (12)$$

with

$$M = 1 + \frac{4(\boldsymbol{k}^\circ\cdot\boldsymbol{\Omega})^2}{(\nu_t k^2 - i\omega)^2}, \quad (13)$$

and

$$D^{(\circ)}_{ij} = M^{-1}\left(\delta_{ij} + \frac{2(\boldsymbol{k}^\circ\cdot\boldsymbol{\Omega})}{\nu_t k^2 - i\omega}\epsilon_{ijs}k^\circ_s\right) \quad (14)$$

as the tensor for a non-magnetised fluid.

It remains to define the original turbulence. We adopt the 'quasi-isotropic' spectral tensor which is identical to that used in Paper I to derive the non-magnetic Λ-effect:

$$\langle\hat{u}^{(0)}_i(\boldsymbol{z},\omega)\,\hat{u}^{(0)}_j(\boldsymbol{z}',\omega')\rangle = \frac{\hat{E}(k,\omega,\boldsymbol{\kappa})}{16\pi k^2}\,\delta(\omega+\omega')\left[\delta_{ij} - \left(1 + \frac{\kappa^2}{4k^2}\right)k^\circ_i k^\circ_j + \frac{1}{2k^2}\left(\kappa_i k_j - \kappa_j k_i\right) + \frac{\kappa_i\kappa_j}{4k^2}\right] \quad (15)$$

where $\boldsymbol{\kappa}$ and $\boldsymbol{k}$ are the wave-vectors for different scales as explained in Paper I.

The $\hat{E}$ is the Fourier transform of the local spectrum,

$$E(k,\omega,\boldsymbol{r}) = \int \hat{E}(k,\omega,\boldsymbol{\kappa})\,e^{ir\kappa}\,d\boldsymbol{\kappa}, \quad (16)$$

hence

$$\langle u'^2\rangle = \int_0^\infty E(k,\omega,\boldsymbol{r})\,dk\,d\omega. \quad (17)$$

Eqs. (6) and (9) can be applied to (15) to find the spectral tensors for rotating and magnetised fluids.

3. Λ-quenching

What we need is the total correlation tensor,

$$Q_{ij}^{\rm tot} = \langle u_i' u_j' \rangle - \langle B_i' B_j' \rangle / \mu\rho, \qquad (18)$$

under the influence of both rotation and large-scale magnetic fields. More definitely, its non-diffusive part which does not vanish for Ω = const. is essential for maintaining of the differential rotation. For simplicity we derive the tensor $Q^{\rm tot}$ for the case of (small-scale) Prandtl number equal unity, $\nu_t = \eta_t$. It is possible also to consider the general case of arbitrary rotation rates and field strengths. We proceed with consideration of simplifying cases. In the following the bar in the symbol for the mean magnetic field is left.

3.1. Slow rotation, arbitrary field strength

Application of (11) to the original turbulence (15) results in

$$\begin{aligned} Q_{ij}^{\rm tot} = & \int_0^\infty \int_0^\infty \frac{\nu_t \, dk d\omega}{\nu_t^2 k^4 + \omega^2} \cdot \frac{\partial^2 E}{\partial x_p \partial x_s} \\ & \Big\{ K_1 \, \Omega_m (\epsilon_{imp}\delta_{js} + \epsilon_{jmp}\delta_{is}) + \\ & + K_2 \frac{\Omega_n B_m}{B^2} (\epsilon_{imp}(B_j\delta_{ns} + B_n\delta_{js}) \\ & + \epsilon_{jmp}(B_i\delta_{ns} + B_n\delta_{is})) + \\ & + K_3 \frac{B_s}{B^2} (\epsilon_{imp}(\Omega_j B_m + \Omega_m B_j) \\ & + \epsilon_{jmp}(\Omega_i B_m + \Omega_m B_i)) + \\ & + K_4 (\boldsymbol{B}\cdot\boldsymbol{\Omega}) \frac{B_m B_s}{B^4} (B_j \epsilon_{imp} + B_i \epsilon_{jmp}) \Big\}. \end{aligned} \qquad (19)$$

The kernels K_n are complicated functions. However, with the simple 'mixing-length' representation for the spectral function,

$$E = 2\,\langle u'^2 \rangle \delta(k - l_{\rm corr}^{-1}) \delta(\omega), \qquad \nu_t = l_{\rm corr}^2 / \tau_{\rm corr}, \qquad (20)$$

(Kitchatinov 1991, $l_{\rm corr}$ and $\tau_{\rm corr}$ as mixing-length and convective turnover time) the K-functions simplify to

$$\begin{aligned} K_1 &= \frac{1}{16\beta^4} \left(\frac{\beta^2+1}{\beta} \arctan\beta - 1 - \frac{2\beta^2}{3(1+\beta^2)} \right), \\ K_2 &= \frac{1}{16\beta^4} \left(5 + \frac{4}{3}\beta^2 - \frac{4\beta^6}{3(1+\beta^2)^2} \right. \\ &\quad \left. - \frac{3\beta^2+5}{\beta} \arctan\beta \right), \\ K_3 &= \frac{1}{16\beta^4} \left(5 + \frac{\beta^2}{3} + \frac{2\beta^4(\beta^2-1)}{3(1+\beta^2)^2} \right. \\ &\quad \left. + \frac{\beta^4 - 2\beta^2 - 5}{\beta} \arctan\beta \right), \\ K_4 &= \frac{1}{16\beta^4} \left(-35 + \frac{22}{3}\beta^2 + \frac{4\beta^4(7\beta^2+3)}{3(1+\beta^2)^3} \right. \\ &\quad \left. - \frac{31\beta^4 + 17\beta^2}{3(1+\beta^2)} + \frac{35 + 10\beta^2 - 3\beta^4}{\beta} \arctan\beta \right). \end{aligned} \qquad (21)$$

With the spectrum (20) the parameter β equals the field strength normalized with the energy equipartition field, i.e.

$$\beta = \frac{|\boldsymbol{B}|}{\sqrt{\mu\rho\langle u'^2\rangle}}. \qquad (22)$$

The dominating component of the large-scale solar magnetic field is the toroidal one. For a purely azimuthal field and $\langle u'^2 \rangle$ only radius-dependent the following representation in spherical geometry is convenient:

$$Q_{r\phi}^{\rm tot} = \nu_T \Omega \sin\theta \, V, \qquad Q_{\theta\phi}^{\rm tot} = \nu_T \Omega \cos\theta \, H, \qquad (23)$$

with

$$\begin{aligned} V &= V^{(0)} + \sin^2\theta \, V^{(1)} + \sin^4\theta \, V^{(2)} \ldots, \\ H &= H^{(0)} + \sin^2\theta \, H^{(1)} + \sin^4\theta \, H^{(2)} \ldots, \end{aligned} \qquad (24)$$

– apart from viscosity terms (Rüdiger 1989).

The V and H are proportional to the functions (21) of the magnetic field. This results in complicated latitudinal dependences of the V and H. We reserve the notations $V^{(n)}$ and $H^{(n)}$ for the parts of V and H which explicitly include the 2n-power of $\sin\theta$. In the series (24), $V^{(0)}$ and $H^{(0)}$ are different from zero:

$$\begin{aligned} V^{(0)} &= \tau_{\rm corr}^2 K_1(\beta) r \frac{\partial}{\partial r} \left(\frac{1}{r} \frac{\partial \langle u'^2 \rangle}{\partial r} \right) + \\ &\quad + \tau_{\rm corr}^2 \left(K_2(\beta) - K_3(\beta) \right) \frac{1}{r} \frac{\partial \langle u'^2 \rangle}{\partial r}, \\ H^{(0)} &= \tau_{\rm corr}^2 K_2(\beta) \frac{\partial^2 \langle u'^2 \rangle}{\partial r^2} - \tau_{\rm corr}^2 K_3(\beta) \frac{1}{r} \frac{\partial \langle u'^2 \rangle}{\partial r}. \end{aligned} \qquad (25)$$

In a further approximation we assume a "short-wave approximation" for $\langle u'^2 \rangle$ in (25) ($r\partial/\partial r \gg 1$) hence

$$V^{(0)} = K_1(\beta) \, \mathscr{G}, \qquad H^{(0)} = K_2(\beta) \, \mathscr{G}, \qquad (26)$$

with

$$\mathscr{G} = \tau_{\rm corr}^2 \frac{\partial^2 \langle u'^2 \rangle}{\partial r^2}. \qquad (27)$$

K_3 does not longer contribute. The appearance of a horizontal component (finite H) of the angular momentum flux in the slow-rotation limit results from the magnetic fields. It is

$$K_1 \simeq \frac{1}{30} - \frac{4\beta^2}{105}, \qquad K_2 \simeq -\frac{8\beta^2}{105} \qquad \text{for} \qquad \beta \ll 1. \qquad (28)$$

The appearance of the new horizontal component of the angular momentum flux shows that the magnetic field does not simply quench the Λ-effect. The $H^{(0)}$-value increases with the magnetic field at small β. In the strong-field limit, however, the Λ-effect is actually suppressed:

$$K_1 \simeq \frac{\pi}{32\beta^3}, \qquad K_2 \simeq -\frac{3\pi}{32\beta^3} \qquad \text{for} \qquad \beta \gg 1. \qquad (29)$$

In Fig. 1 the magnetic field-dependences of the quenching functions for all values of β are shown.

3.2. Weak field, arbitrary rotation rate

The non-magnetic Λ-effect for the same turbulence model was derived in Paper I. Here we consider the B^2-corrections of the resulting Reynolds stresses. Application of (12) to (9) and (15) results in

$$
\begin{aligned}
Q_{ij}^{\rm tot} &= \int_0^\infty\int_0^\infty \frac{\nu_t\beta^2\,dkd\omega}{\nu_t^2k^4+\omega^2}\Big\{\\
&+ J_1(\Omega_m+2\frac{(\boldsymbol{\Omega}\cdot\boldsymbol{B})}{B^2}B_m)(\epsilon_{imp}\delta_{js}+\epsilon_{jmp}\delta_{is})+\\
&+ \frac{J_2\Omega_s}{\Omega^2}\Big[(\Omega_j\Omega_m+2\frac{(\boldsymbol{\Omega}\cdot\boldsymbol{B})}{B^2}(B_j\Omega_m+B_m\Omega_j))\epsilon_{imp}\\
&\quad+(\Omega_i\Omega_m+2\frac{(\boldsymbol{\Omega}\cdot\boldsymbol{B})}{B^2}(B_i\Omega_m+B_m\Omega_i))\epsilon_{jmp}\Big]\\
&+ J_3\frac{B_s}{B^2}((\Omega_jB_m+\Omega_mB_j)\epsilon_{imp}+\\
&\quad+(\Omega_iB_m+\Omega_mB_i)\epsilon_{jmp})\\
&+ J_4\frac{\Omega_sB_m}{B^2}(B_j\epsilon_{imp}+B_i\epsilon_{jmp})+\\
&+ J_5\frac{(\boldsymbol{\Omega}\cdot\boldsymbol{B})B_s\Omega_m}{\Omega^2B^2}(\Omega_j\epsilon_{imp}+\Omega_i\epsilon_{jmp})+\\
&+ J_6\frac{(\boldsymbol{\Omega}\cdot\boldsymbol{B})^2\Omega_m}{\Omega^2B^2}(\epsilon_{imp}\delta_{js}+\epsilon_{jmp}\delta_{is})+\\
&+ J_7\frac{(\boldsymbol{\Omega B})^2\Omega_m\Omega_s}{\Omega^4B^2}(\Omega_j\epsilon_{imp}+\Omega_i\epsilon_{jmp})\Big\}\frac{\partial^2E}{\partial x_p\partial x_s}. \qquad (30)
\end{aligned}
$$

For the single-scale spectrum (20) the kernels are simple enough to give their complete expressions,

$$
\begin{aligned}
J_1 &= \frac{1}{8\Omega^{*6}}\Big(10-\frac{13}{3}\Omega^{*2}-\frac{2\Omega^{*2}}{1+\Omega^{*2}}+\\
&\quad+\frac{\Omega^{*4}+3\Omega^{*2}-10}{\Omega^*}\arctan\Omega^*\Big),\\
J_2 &= \frac{1}{32\Omega^{*6}}\Big(-280+\frac{235}{3}\Omega^{*2}-21\Omega^{*4}+\frac{24\Omega^{*6}}{1+\Omega^{*2}}+\\
&\quad+\frac{3\Omega^{*6}-30\Omega^{*4}+15\Omega^{*2}+280}{\Omega^*}\arctan\Omega^*\Big),\\
J_3 &= \frac{1}{4\Omega^{*6}}\Big(10-\frac{\Omega^{*2}}{3}+\frac{\Omega^{*4}-3\Omega^{*2}-10}{\Omega^*}\arctan\Omega^*\Big),\\
J_4 &= \frac{1}{16\Omega^{*6}}\Big(40-\frac{31}{3}\Omega^{*2}-3\Omega^{*4}-\\
&\quad-\frac{3\Omega^{*6}-10\Omega^{*4}+3\Omega^{*2}+40}{\Omega^*}\arctan\Omega^*\Big),\\
J_5 &= \frac{1}{4\Omega^{*6}}\Big(-70+\frac{25}{3}\Omega^{*2}-\frac{6\Omega^{*4}}{1+\Omega^{*2}}-\\
&\quad-\frac{3\Omega^{*4}-15\Omega^{*2}-70}{\Omega^*}\arctan\Omega^*\Big),\\
J_6 &= \frac{1}{8\Omega^{*6}}\Big(-70+\frac{55}{3}\Omega^{*2}-\frac{4\Omega^{*2}}{(1+\Omega^{*2})^2}+\\
&\quad+\frac{24\Omega^{*2}}{1+\Omega^{*2}}-\frac{3\Omega^{*4}+15\Omega^{*2}-70}{\Omega^*}\arctan\Omega^*\Big),
\end{aligned}
$$

$$
\begin{aligned}
J_7 &= \frac{3}{32\Omega^{*6}}\Big(840-245\Omega^{*2}-3\Omega^{*4}-\\
&\quad-\frac{16\Omega^{*4}}{(1+\Omega^{*2})^2}+\frac{376\Omega^{*4}}{3(1+\Omega^{*2})}-\\
&\quad-\frac{3\Omega^{*6}-50\Omega^{*4}+35\Omega^{*2}+840}{\Omega^*}\arctan\Omega^*\Big), \qquad (31)
\end{aligned}
$$

where $\Omega^*=2\tau_{\rm corr}\Omega$ is the Coriolis number.

For an azimuthal magnetic field and only radial inhomogeneities we find for the functions V and H in (24)

$$
\begin{aligned}
V^{(0)} &= \beta^2\tau_{\rm corr}^2\left(J_1(\Omega^*)+J_2(\Omega^*)\right)r\frac{\partial}{\partial r}\frac{1}{r}\frac{\partial\langle u'^2\rangle}{\partial r}+\\
&\quad+\beta^2\tau_{\rm corr}^2\left(J_4(\Omega^*)-J_3(\Omega^*)\right)\frac{1}{r}\frac{\partial\langle u'^2\rangle}{\partial r},\\
V^{(1)} &= -\beta^2\tau_{\rm corr}^2J_2(\Omega^*)r\frac{\partial}{\partial r}\left(\frac{1}{r}\frac{\partial\langle u'^2\rangle}{\partial r}\right),\\
H^{(0)} &= \beta^2\tau_{\rm corr}^2\left(J_4(\Omega^*)\frac{\partial^2\langle u'^2\rangle}{\partial r^2}-J_2(\Omega^*)\frac{1}{r}\frac{\partial\langle u'^2\rangle}{\partial r}\right),\\
H^{(1)} &= V^{(1)}. \qquad (32)
\end{aligned}
$$

The short-wave approximation now yields

$$
\begin{aligned}
V^{(0)} &= \beta^2\,\mathscr{G}\left(J_1(\Omega^*)+J_2(\Omega^*)\right),\quad V^{(1)}=-\beta^2\,\mathscr{G}J_2(\Omega^*)\\
H^{(0)} &= \beta^2\,\mathscr{G}J_4(\Omega^*),\qquad\qquad H^{(1)}=-\beta^2\,\mathscr{G}J_2(\Omega^*). \qquad (33)
\end{aligned}
$$

Only three functions of the Coriolis number form the magnetic corrections to the angular momentum fluxes. The limits of these functions for slow rotation ($\Omega^*\ll1$) reproduce the expressions (26) and (28):

$$J_1=-4/105,\quad J_4=-8/105,\quad J_2=O(\Omega^{*2}). \qquad (34)$$

For the opposite case of rapid rotation we find

$$J_2=3\pi/(64\Omega^*),\quad J_4=-2J_2,\quad J_1=O(\Omega^{*-3}). \qquad (35)$$

It can be shown that for rapid rotation the contributions of the density gradient (neglected above) and the turbulence intensity gradient always combine into common gradients. Eq. (27) can thus be replaced by

$$\mathscr{G}=\frac{\tau_{\rm corr}^2}{\rho^2}\frac{\partial^2\left(\rho^2\langle u'^2\rangle\right)}{\partial r^2} \qquad (36)$$

to get the result for rapid rotation including the effect of the density stratification,

$$
\begin{aligned}
V^{(0)} &= -\frac{\pi\mathscr{G}}{16\Omega^*}\left(1-\frac{3}{4}\beta^2\right),\qquad H^{(0)}=-\beta^2\frac{3\pi\mathscr{G}}{32\Omega^*},\\
V^{(1)} &= H^{(1)}=-V^{(0)}, \qquad (37)
\end{aligned}
$$

where the non-magnetic contributions are also included. Note the negativity of the product of the fluxes $H^(0)$ and $H^(1)$.

4. Dynamo model

A simple 1D nonlinear dynamo model is considered for the consequences of the nonlinear Λ-effect for stellar dynamos. The model is similar to that by Schmitt & Schüssler (1989) and shall be understood as a simplified version of the overshoot layer dynamo. The very new ingredient of our approach is the inclusion of the equation of motion.

We neglect the radial dimension to get the (normalized) field equations,

$$\begin{aligned}\frac{\partial A}{\partial t} &= \cos\theta\,\Phi_\alpha(B)B + \frac{\partial}{\partial\theta}\left(\frac{1}{\sin\theta}\frac{\partial}{\partial\theta}\sin\theta A\right),\\ \frac{\partial B}{\partial t} &= -\mathscr{D}\,\tilde{\Omega}(\theta)\frac{\partial(\sin\theta A)}{\partial\theta} + \frac{\partial}{\partial\theta}\left(\frac{1}{\sin\theta}\frac{\partial}{\partial\theta}\sin\theta B\right),\end{aligned} \quad (38)$$

where $\mathscr{D}$ is the dynamo number, A is the poloidal field potential, B is the normalized toroidal field, $\Phi_\alpha(B)$ is the α-effect quenching function, and $\tilde{\Omega}(\theta) = \Omega_0^{-1}\,\partial\Omega/\partial x$ is the normalized radial shear, which is both latitude- and time-dependent. In the sense of an $\alpha\Omega$-dynamo we kept the α-effect only in the poloidal field equation. The α-effect is supposed to vary as $\cos\theta$ with latitude.

The equation for the shear, $\tilde{\Omega}$, must be derived from the angular momentum equation (cf. Rüdiger 1989),

$$\begin{aligned}\frac{\partial\Omega}{\partial t} &= \frac{1}{\rho r^4}\frac{\partial}{\partial r}\left(\nu_T\rho r^3\left[r\frac{\partial\Omega}{\partial r} - \Omega_0 V\right]\right) +\\ &+ \frac{\nu_T}{r^2\sin^3\theta}\frac{\partial}{\partial\theta}\left(\sin^2\theta\left[\sin\theta\frac{\partial\Omega}{\partial\theta} - \Omega_0 H\cos\theta\right]\right),\end{aligned} \quad (39)$$

where V and H are defined by (24). Note that under the approximations leading to (39) the mean-field Lorentz force does not contribute. We assume further a simple power-law dependence on the fractional radius, $x = r/R$, for the viscosity and the H-function: $\nu_T = \tilde{\nu}x^2$ and $H = \tilde{H}x$. Under these assumptions the 1D equation for the shear $\tilde{\Omega}$ is

$$\frac{\partial\tilde{\Omega}}{\partial t} = \frac{\mathrm{Pm}}{\sin^3\theta}\frac{\partial}{\partial\theta}\left[\sin^2\theta\left(\sin\theta\,\frac{\partial\tilde{\Omega}}{\partial\theta} - \cos\theta\tilde{H}\right)\right], \quad (40)$$

where t is again normalized with the diffusion time, Pm is the magnetic Prandtl number, $\mathrm{Pm} = \tilde{\nu}/\eta_T$, and the radial dimension is neglected as in (38). We modify the representation (24) for the function H,

$$\tilde{H} = \tilde{H}^{(1)}(0)\left(\Phi_0(B) + \sin^2\theta\,\Phi_1(B)\right). \quad (41)$$

Φ_1 is thus normalized to $\Phi_1(0) = 1$ and can be understood as a quenching function for $H^{(1)}$. Accordingly it is $\Phi_0(B) = H^{(0)}(B)/H^{(1)}(0)$. If the shear $\tilde{\Omega}$ is measured in units of the (positive) $\tilde{H}^{(1)}(0)$, Eq. (40) becomes

$$\begin{aligned}\frac{\partial\tilde{\Omega}}{\partial t} &= \frac{\mathrm{Pm}}{\sin^3\theta}\frac{\partial}{\partial\theta}\left[\sin^2\theta\left(\sin\theta\,\frac{\partial\tilde{\Omega}}{\partial\theta} +\right.\right.\\ &\left.\left. - \left(\cos\theta\,\Phi_0(B) + \cos\theta\sin^2\theta\,\Phi_1(B)\right)\right)\right].\end{aligned} \quad (42)$$

Then the dynamo number, $\mathscr{D}$, is defined as

$$\mathscr{D} = -\frac{\Omega_0\tilde{H}^{(1)}(0)\,\alpha R^3}{\eta_T^2}. \quad (43)$$

Eq. (42) satisfies the shear-conservation law, i.e. the integral shear,

$$S = \int_0^\pi \tilde{\Omega}(\theta)\sin^3\theta\,d\theta, \quad (44)$$

does not change with time.

Eqs. (38) and (42) provide a closed system for both the magnetic field and the shear. The usual boundary conditions imposed on this system are

$$A = B = \partial\tilde{\Omega}/\partial\theta = 0 \quad \text{for } \theta = 0, \pi. \quad (45)$$

With these conditions the shear is free of an arbitrary constant. It can be fixed to zero with the additional condition for rigid rotation,

$$\lim_{\beta\to\infty}\tilde{\Omega} = 0, \quad (46)$$

or – which is the same – by equating the integral (44) to zero:

$$S = 0. \quad (47)$$

With any other choice, the $\tilde{\Omega}$ tends to a latitude-independent constant for a very strong field.

It remains to fix the quenching functions. For the α-quenching the relation

$$\Phi_\alpha(\beta) = \frac{15}{32\beta^4}\left(1 - \frac{4\beta^2}{3(1+\beta^2)^2} - \frac{1-\beta^2}{\beta}\arctan\beta\right) \quad (48)$$

is used from Rüdiger & Kitchatinov (1993).

Section 3 supplies the complete quenching functions for only $H^{(0)}$ and $V^{(0)}$. For $H^{(1)}$ the quenching function is not well-known. We adopt K_1 for the latter as it is in agreement with the results in Eq. (37). The functions are then rescaled to satisfy $\Phi_1(0) = 1$:

$$\Phi_0(\beta) = 30K_2(\beta), \quad \Phi_1(\beta) = 30K_1(\beta). \quad (49)$$

The β-dependences of the functions (48) and (49) are shown in Fig. 1.

The quenching function K_1 is *adopted* in (49) for the horizontal Λ-effect. This is not a final procedure. We have, however, actually derived quenching functions for all the effects involved in our dynamo model for the case of weak magnetic field (the β^2-corrections, Eq. (37)). For the rapid-rotation case, to which the solar-type stars belong, they read

$$\Phi_\alpha = 1 - 3\beta^2/2, \quad \Phi_0 = -3\beta^2/2, \quad \Phi_1 = 1 - 3\beta^2/4. \quad (50)$$

The nonlinear simulations below are made with the quenching (50) also to find that within its validity region it produces essentially the same results as obtained with (48) and (49).

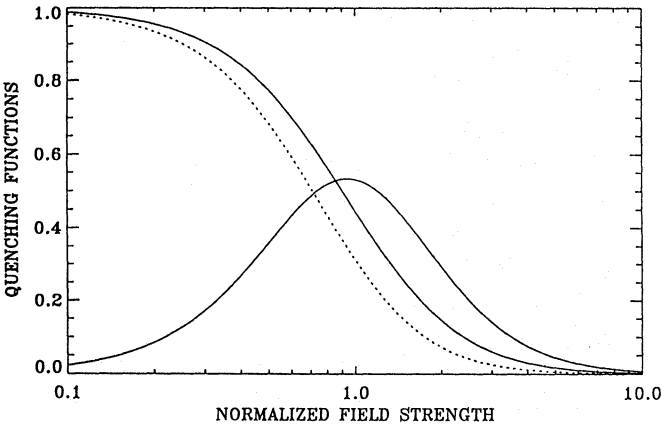

Fig. 1. The quenching functions (48) and (49) for the α-effect (dashed) and the Λ-effect (solid). The negative value of $\Phi_0(\beta)$ is plotted. Λ-quenching is stronger

4.1. Linear properties

We consider first the linear properties of the model. The shear profile,

$$\tilde{\Omega}(\theta) = \frac{1}{10}(5\sin^2\theta - 4) \tag{51}$$

is the steady solution of the (non-magnetic) Eq. (42) satisfying the conditions (45) and (47). The profile (51) describes a weak positive shear (super-rotation) at the equator and more pronounced sub-rotation at high latitudes similar to the findings of helioseismology for the base of the solar convection zone.

As usual (cf. Schmitt & Schüssler 1989) the linear problem was treated as an eigenvalue problem, $A, B \sim e^{i\omega_{\rm cyc}t}$ ($\omega_{\rm cyc}$ is now *complex*). The θ-dependences are described by the series expansions in Legendre polynomials,

$$A = e^{i\omega_{\rm cyc}t}\sum a_n\, P_n^1(\cos\theta),$$
$$B = e^{i\omega_{\rm cyc}t}\sum b_n\, P_n^1(\cos\theta). \tag{52}$$

The dependence of the growth rate, $-\Im(\omega_{\rm cyc})$, of both dipole parity (odd a_n and even b_n) and quadrupole parity (even a_n and odd b_n) modes on the (negative) dynamo number, $\mathscr{D}$ is computed with the truncation level $n = 30$ in the expansions (52). The threshold dynamo numbers for the dipole parity ($\simeq -5630$) and the quadrupole parity ($\simeq -5650$) are very close together. Both modes are oscillatory, $\Re(\omega_{\rm cyc}) \neq 0$.

For positive dynamo numbers, on the contrary, the first modes becoming growing are the steady quadrupole ($\mathscr{D}_{\rm crit} \simeq 170$) and the steady dipole ($\mathscr{D}_{\rm crit} \simeq 247$).

Positive and negative critical dynamo numbers differ in their absolute values by more than one order of magnitude. This is rather unusual. Usually one finds 'parity symmetry': the modes with dipole and quadrupole parities exchange their eigenvalues when the sign of the dynamo number is changed. This rule is here strongly violated. The reason is that the symmetry holds only for latitude-independent shear which is not realized with the present model.

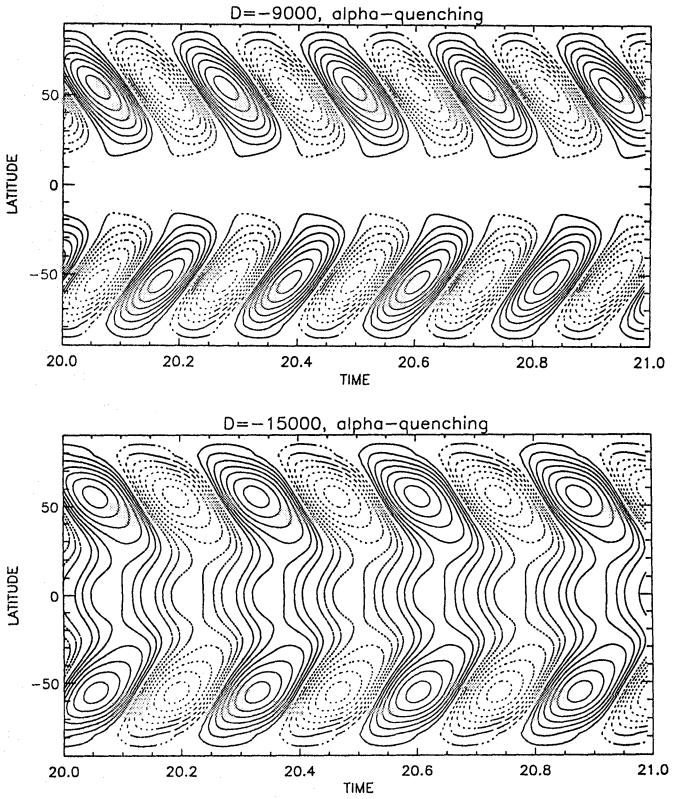

Fig. 2. Butterfly diagrams for the dipole parity (top) and quadrupole parity (bottom) solutions of the model without Λ-quenching

4.2. α-quenching

Negative dynamo numbers are preferred because this sign is expected for the Sun and positive dynamo numbers lead to steady solutions.

The computations are for 2 approaches – with full nonlinearity and without Λ-quenching. Only oscillatory solutions are found for the α-quenching model (Fig. 3). Just beyond the threshold dynamo number ($\mathscr{D} \simeq -5630$) the oscillating dipole-parity solution appears. It survives until $|\mathscr{D}| \simeq 12\,800$. For $|\mathscr{D}| > 13\,700$ the parity changes to an oscillating quadrupole. It is present until $|\mathscr{D}| = 120\,000$ beyond which we did not follow the model. The transition region $12\,800 < |\mathscr{D}| < 13\,700$ produces mixed-parity oscillations.

4.3. Full nonlinearity

The fully nonlinear model has a wider variety of solutions. For small dynamo numbers, i.e. $|\mathscr{D}| < 6050$ we find surprisingly mixed-parity two-torus oscillations.

Fig. 3 shows the time-dependences of the maximum of B^2 and the parity index

$$P = \frac{E_q - E_d}{E_q + E_d} \tag{53}$$

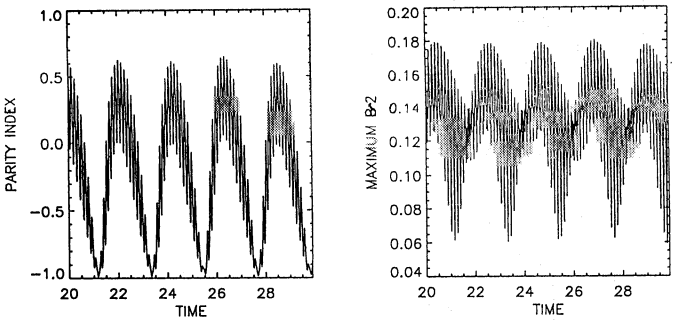

Fig. 3. The parity index (left) and the maximal B^2-value for $\mathscr{D} = -6000$ in the fully nonlinear model (Pm = 1)

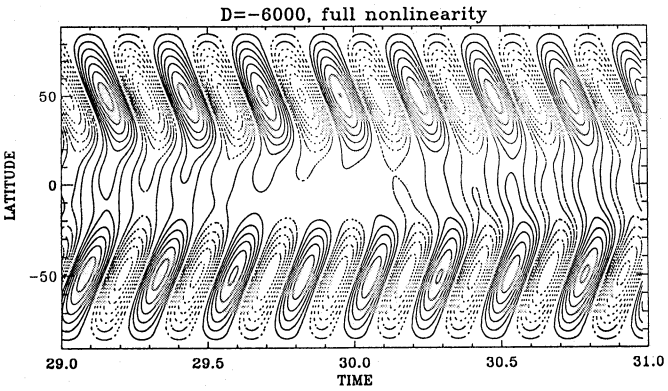

Fig. 4. The butterfly diagram for the mixed-parity two-torus solution

(Brandenburg et al.1989), where E_q and E_d are the 'total energies',

$$E_{d,q} = \int_0^\pi B^2_{d,q}(\theta) \sin\theta \, d\theta, \qquad (54)$$

for the quadrupole, $B_q(\theta) = (B(\theta) - B(\pi-\theta))/2$, and the dipole, $B_d(\theta) = (B(\theta) + B(\pi-\theta))/2$, components of the total toroidal field, $B = B_q + B_d$. The short-term oscillations ($t_{\rm osc} \sim 0.2$) are modulated with a long ($t \sim 2$) period with dipolar and quadrupolar parities alternatively prevailing. The butterfly diagram for the two-torus solution is given in Fig. 4. Fig. 5 shows the temporal variations of the equatorial shear, $\tilde{\Omega}(\pi/2)$. Short-term 'torsional oscillations' with amplitude of about 1% are present together with the stronger ($\sim$ 5%) long-term modulation. After the Figs. 3 and 5 the long-term oscillations of the maximum B^2 and the shear are in anti-phase.

A long-term beat phenomenon was also found by Brandenburg et al. (1989) in a 2D fully-convective sphere with α-quenching. The result is interpreted as due the fact that the critical dynamo numbers for the quadrupole and dipole symmetry are close together. The beat phenomenon of the present model, however, has quite a different origin. It does not exist without the Λ-quenching effect. The long-term beats result from phase interactions between magnetic field and the differential rotation. For too high dynamo numbers, i.e. too strong magnetic fields, the magnetic feedback to the rotational shear is so strong that the rotation law changes its character (in particular at the poles) and, consequently, the dynamo switches to another regime.

In the region $6050 < |\mathscr{D}| < 6350$ an oscillatory quadrupole-parity solution very similar to that of the α-quenching model (Fig. 2) is found. This solution is replaced at $|\mathscr{D}| \simeq 6350$ by steady quadrupole which survives until a rather large dynamo number of about −73 000.

4.4. Magnetic Prandtl number

The above results concern turbulences with Pm=1. Smaller values, however, are more realistic. As indicated in Eq. (40) the magnetic Prandtl number directs the phase relation between field and flow. For large Pm field and flow tend to be in phase while for small Pm the rule is to be out of phase.

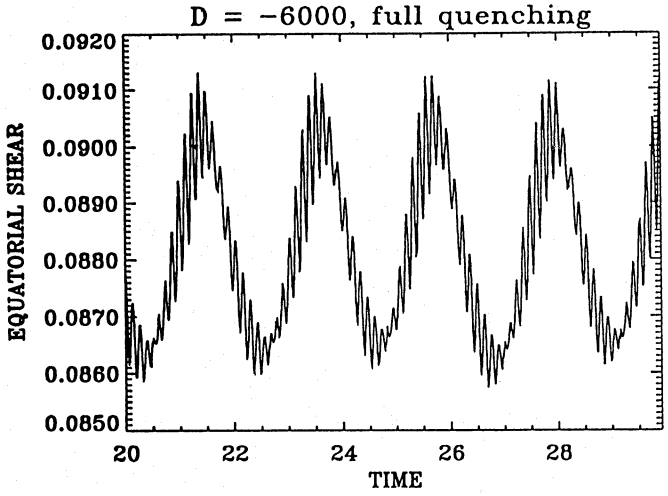

Fig. 5. Time-dependence of the equatorial shear, $\tilde{\Omega}(\pi/2)$, of the two-torus solution. After (56) also the evolution of the equatorial angular velocity is yielded

The effect for the dynamo system is strong. The phenomena described above for Pm = 1 are also existing for Pm = 0.1 but with higher amplitudes. Tab. 1 reveals the trends.

Models of the first two lines have weak magnetic fields. The rotation law keeps its original shape. The weak-field case ($\mathscr{D} = -6000$) exhibits 3 frequencies with mixed parity. For higher fields ($\mathscr{D} = -8000$) only 1 frequency survives with constant (quadrupole) parity.

If the dynamo number is further increased the polar shear changes its sign. The sub-rotation ($\partial\Omega/\partial r < 0$) in the polar region becomes a super-rotation ($\partial\Omega/\partial r > 0$) – as it exists in the equatorial region, too. At the same time, the magnetic activity looses its simple cyclic character. Its power spectrum exhibits a great sample of frequencies (Fig. 6), close to a chaotic behaviour.

For even stronger fields the rotation law totally changes its character. The equatorial super-rotation becomes an equatorial sub-rotation, and the polar sub-rotation becomes a polar super-rotation. Apparently the dynamo number itself changes its sign and the final result is a steady quadrupole.

Table 1. Summary of characteristics of models for increasing magnetic field strength (Pm = 0.1). See the text for details

$-\mathscr{D}$	$\beta_{\max}$	cycles	parity	$\tilde{\Omega}_{\rm pole}$	$\tilde{\Omega}_{\rm eq}$
6000	0.3	3	$-1 \ldots +1$	~ -0.34	~ 0.09
8000	0.4	1	1	~ -0.20	~ 0.07
18 000	0.6	chaos?	$-1 \ldots +1$	$0 \ldots 1$	~ 0.05
24 000	3	0	1	~ 1	~ -0.02

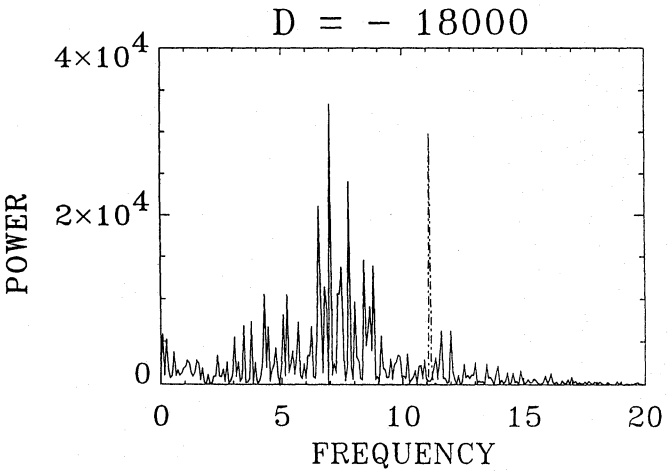

Fig. 6. Power spectrum of the magnetic field variations for intermediate dynamo numbers ($\mathscr{D} = -18\,000$). The dashed line gives the power spectrum with Λ-quenching ignored

5. Discussion

Dynamo theory considers flow fields in plasma inducing large-scale magnetic fields. The magnetic feedback on the flow defines the nonlinear dynamo with basically new features compared with the linear, kinematic theory.

So far, we are familiar with 3 feedback mechanisms: α-quenching, Λ-quenching and the Malkus-Proctor effect. All of them seem to produce long-term modulations of the basic activity cycle which are observed in form of the Maunder minimum and the long-term monitoring of chromospheric activity. 15% of the observed stars exhibit a uniform Ca II emission on a rather low level (Saar & Baliunas 1993). Whether the Malkus-Proctor effect really provides a temporal modulation is still under debate (Hollerbach 1991). Both Malkus-Proctor effect and Λ-quenching are producing a cyclic variation of the rotation law such as observed as the solar torsional oscillations.

The solution illustrated by the Figs. 3 to 5 closely resembles the basic solar observations. The short-term variations of the differential rotation (Fig. 5) can be identified with the solar torsional oscillations (Howard & LaBonte 1980). The rotation law at the surface is simply

$$\Omega_{\rm surf}(\theta) = \left(1 + \tilde{H}^{(1)}(0)\ \tilde{\Omega}(\theta)\right)\ \Omega_0. \qquad (55)$$

In Fig. 5 the equatorial angular velocity is given. Comparison with Fig. 3 shows that the cycle level and equatorial rotation are in anti-phase: maximum cycles are related to minimum equatorial rotation and v.v. Only the minimum cycles have a distinct dipolar parity. The "resting cycles" with the smallest amplitudes of the short-term oscillations and minimal peak-values of B^2 show a clear dominance of quadrupolar parity.

Verma (1993) reported long-term ($\sim$ 110 yrs) variations in the N-S-asymmetry of the solar activity similar to Fig. 4. Yoshimura & Kambry (1993 a,b) found the 100 yr modulation of the solar cycle indeed correlated with long-term variations of the differential rotation. Maximum magnetism is correlated with maximum equatorial rotation and minimum differential rotation ("fast and rigid"). For the Maunder minimum Ribes & Nesme-Ribes (1993) found correspondingly slow equatorial rotation and strong differential rotation ("slow and steep"). The global minima may be identified with the "resting cycles" of the present model. The equatorial rotation (Fig. 5) is on the descending branch of its long-term variations at these epochs. The fastest rotation coincides with the beginning of the resting-cycles periods.

It would be too optimistic, however, to explain the Maunder minimum by the Λ-quenching formulation after the presented simple 1D model. More work in this direction is suggested.

Acknowledgements. L.L.K. thanks for the support by the Alexander von Humboldt Foundation. The authors are grateful to A. Brandenburg for a critical reading of the manuscript.

References

Brandenburg A., Krause F., Meinel R., Moss D., Tuominen I., 1989, A&A 213, 411
Brandenburg A., Meinel R., Moss D., Tuominen I., 1990, in: Solar Photosphere: Structure, Convection, and Magnetic Fields, ed. J.O. Stenflo, p. 379
Hollerbach R., 1991, Geophys. Astrophys. Fluid Dyn. 60, 245
Howard R., LaBonte B. J., 1980, ApJ 239, L33
Jennings R. L., Weiss N. O., 1991, MNRAS 252, 249
Kitchatinov L. L., 1990, Geophys. Astrophys. Fluid Dyn. 54, 145
Kitchatinov L. L., 1991, A&A 243, 483
Kitchatinov L. L., Rüdiger G., 1993, A&A 276, 96 (Paper I)
Malkus W. V. R., Proctor M. R. E., 1975, J. Fluid Mech. 67, 417
Noyes R. W., Weiss N. O., Vaughan A. H., 1984, ApJ 287, 769
Parker E. N., 1979, Cosmic magnetic fields, Clarendon Press, Oxford
Ribes J. C., Nesme-Ribes E., 1993, A&A 276, 549
Rüdiger G., 1989, Differential rotation and stellar convection: Sun and solar-type stars, Gordon and Breach Science Publishers, New York
Rüdiger G., Kitchatinov L. L., 1990, A&A 236, 503
Rüdiger G., Kitchatinov L. L., 1993, A&A 269, 581
Saar S. H., Baliunas S. L., 1993, in: The Solar Cycle Workshop, ed. K. L. Harvey, ASP Conf. Series 27
Schmitt D., Schüssler M., 1989, A&A 223, 343
Spörer G., 1889, Verhandl. Kgl. Leopold.-Carol. Deutschen Akad. Naturf. 53, 283
Stenflo J. O., Vogel M., 1986, Nat 319, 285
Verma V. K., 1993, ApJ 403, 797
Yoshimura H., Kambry M. A., 1993a, Astron. Nachr. 314, 9
Yoshimura H., Kambry M. A., 1993b, Astron. Nachr. 314, 21